balt6/z7l-ir/z7l-ir/z7l00610/z7l3090-10z | xppws | S=1 | 4/2/10 | 3:36 | 4/Color Figure(s): F1-3 | Art: RLI200544

AQ:1

Adenosine-Stress Dynamic Myocardial CT Perfusion Imaging

Initial Clinical Experience

Gorka Bastarrika, MD, PhD,† Luis Ramos-Duran, MD,* Michael A. Rosenblum, MD,‡ Doo Kyoung Kang, MD,*§ Garrett W. Rowe, BS,* and U. Joseph Schoepf, MD*‡*

Objective: To evaluate the feasibility of adenosine-stress dynamic myocardial volume perfusion imaging with dual source computed tomography (CT) for the qualitative and quantitative assessment of myocardial blood flow (MBF) compared with stress perfusion and viability magnetic resonance imaging (MRI).

Material and Methods: Ten patients (8 male, 2 female, mean age 62.7 ± 7.1 years) underwent stress/rest perfusion and delayed-enhancement MRI, and a cardiac CT protocol comprising prospectively electrocardiogram -triggered coronary CT angiography, dynamic adenosine-stress myocardial perfusion imaging using a "shuttle" mode, and delayed enhancement acquisitions. Two independent observers visually assessed myocardial perfusion defects. For semi-quantitative evaluation, CT- and MRI-derived myocardial-to-left ventricular upslope indices were compared. Additionally, absolute MBF was quantified based on dynamic perfusion CT and correlated with semi quantitative CT measurements. Myocardial perfusion analysis was performed on a segmental basis. Analysis used paired *t* tests, Wilcoxon signed-rank test, linear correlation, and Bland-Altman statistics.

Results: A total of 149 segments (93.1%) were suitable for analysis. Sensitivity, specificity, positive and negative predictive values for detection of myocardial perfusion defects at CT compared with MRI were 86.1%, 98.2%, 93.9%, and 95.7%, respectively. Semiquantitative analysis of CT data showed significant differences between ischemic and nonischemic myocardium with a signal intensity upslope that was comparable with MRI-derived values (CT: 5.2 ± 2 SI/s, MRI: 4.8 ± 2.3 SI/s, $P > 0.05$). Moderate correlation was observed between absolute CT quantification of MBF and semi-quantitative CT measurements. Mean total dose length product for the entire cardiac CT protocol was 1290.4 ± 233.3 mGy cm.

Conclusion: Adenosine-stress volumetric first pass CT perfusion imaging is feasible and may enable the evaluation of qualitative and semi quantitative parameters of myocardial perfusion in a comparable fashion as MRI.

Key Words: computed tomography, coronary vessels, angiography, myocardial perfusion

(*Invest Radiol* 2010;45: 000–000)

In clinical practice, the physiological significance of coronary artery stenosis is ordinarily assessed with myocardial perfusion imaging modalities during pharmacologically induced hyperemia. Single photon emission computed tomography[1] is the most widely used modality, although cardiac magnetic resonance imaging (MRI)[2] has demonstrated its superiority for detecting nontransmural perfusion defects mainly because ofits higher spatial resolution.[3]

The usefulness of multi detector-row CT (MDCT) for ruling out significant coronary artery stenosis[4–6] and for providing prognostic information in patients with suspected coronary artery disease[7–10] has repeatedly been demonstrated. Moreover, recent literature suggests the feasibility of using MDCT as a standalone technology for integrative evaluation of coronary heart disease.[11–15] The standard spiral acquisition mode of MDCT, however, cannot dynamically evaluate the time-resolved passage of contrast medium through the myocardium and thus provides only limited information on the hemodynamic consequences of coronary artery disease.

The greater detector coverage of a recently introduced dual-source CT (DSCT) system[16,17] may enable the performance of dynamic myocardial volume perfusion imaging of the heart by means of a dedicated "shuttle" mode, comprising rapid electrocardiogram (ECG)-triggered image acquisition at 2 alternating table positions during contrast medium infusion. This investigation aimed at determining the feasibility of applying this technique for the qualitative and (semi) quantitative CT assessment of myocardial perfusion during adenosine stress using stress/rest perfusion and delayed enhancement MRI as the reference standard.

MATERIALS AND METHODS

The study protocol was approved by our institutional review board and all patients gave written informed consent. Ten consecutive symptomatic subjects with known or high likelihood of coronary artery disease prospectively underwent stress/rest perfusion and delayed enhancement MRI and stress-perfusion and delayed enhancement cardiac CT. Subjects with known contrast media allergy, impaired renal function (creatinine >1.5 mg/dL), arrhythmia (eg, atrial fibrillation), claustrophobia, or MRI-incompatible implanted devices were excluded from participation. All subjects underwent both procedures within 24 hours.

Cardiac MRI Acquisition Protocol

MRI studies were performed using a 1.5-T system (Magnetom Avanto, Siemens, Erlangen, Germany) using a 6-element phased array coil. Stress perfusion MRI was performed 3 minutes into the intravenous infusion of adenosine (140 μg/kg/min Adenoscan, Astellas, Tokyo, Japan) using steady-state free precession (SSFP, TrueFISP Siemens) perfusion sequences. Three short axis sections representative of basal, mid, and apical myocardial portions were acquired with the following parameters: repetition time (TR) 2.8 ms, echo time (TE) 1.21 ms, flip angle 50°, field of view 380 × 80.2 mm, matrix 116 × 192, acquisition duration 150 ms per slice, slice thickness 10 mm, 50 measurements, and an acceleration factor of 2 (GRAPPA, Siemens). Ten minutes after stress perfusion, rest perfusion images were obtained in the same technique. Contrast enhancement during stress and rest perfusion MRI was accomplished with gadopentetate dimeglumine (Magnevist, Bayer-Schering, Berlin, Germany; 0.05 mmol/kg each for rest and stress MRI

Received December 10, 2009; accepted for publication (after revision) February 15, 2010.

From the *Department of Radiology and Radiological Science, Medical University of South Carolina, Charleston, SC; †Department of Radiology, University of Navarra, Pamplona, Spain; ‡Division of Cardiology, Department of Medicine, Medical University of South Carolina, Charleston, SC; and §Department of Radiology, Ajou University Hospital, Suwon, South Korea.

Supported by Bayer-Schering, Bracco, General Electric, Medrad, and Siemens (to U.J.S.).

G.B. is a consultant for General Electric, Medrad, and Siemens. U.J.S. is a consultant.

Reprints: U. Joseph Schoepf, MD, Department of Radiology and Radiological Science, Medical University of South Carolina, Ashley River Tower, 25 Courtenay Dr, MSC 226, Charleston, SC 29401. E-mail: schoepf@musc.edu.

ISSN: 0020-9996/10/4506-0001

balt6/z7l-ir/z7l-ir/z7l00610/z7l3090-10z | xppws | S=1 | 4/2/10 | 3:36 | 4/Color Figure(s): F1-3 | Art: RLI200544

perfusion imaging, 0.1 mmol/kg total), injected at 4 mL/s followed by 15 mL of normal saline. In addition, functional analysis was performed with retrospectively ECG-gated 8 mm slice-thickness cine loops in short and long axis views using a SSFP sequence (TR: 3.09 ms, TE: 1.3 ms, flip angle 80°, field of view 280 × 375 mm, matrix 156 × 192, 25 phases per cardiac cycle, no interslice gap, in-plane resolution 1.7 × 1.7 mm). Finally, delayed images were acquired using a phase sensitive inversion-recovery SSFP sequence (TR: 3.38 ms, TE: 1.4 ms, flip angle 45°, field of view: 340 × 68.8 mm, matrix 127 × 256, slice thickness 8 mm, no interslice gap).

Cardiac CT Acquisition Protocol

All patients underwent cardiac CT using a DSCT system (SOMATOM Definition Flash, Siemens). Initially, single heart-beat CT calcium scoring was acquired with the following parameters: 2 × 64 × 0.6 mm detector collimation resulting in 2 × 128 × 0.6 mm sections by means of the *z*-flying focal spot technique, 280 ms gantry rotation time, 120 kV tube potential, and 73 mAs per rotation tube current time product. Subsequently prospectively ECG-triggered coronary CT angiography was performed. Contrast medium enhancement was achieved using a triphasic injection protocol with injection of 70 mL of pure, undiluted iodinated contrast material (iopromide, Ultravist 370 mgI/mL, Bayer-Schering) followed by a constant volume of 50 mL of a 70%:30% saline-to-contrast medium mixture and 30 mL of pure saline, all injected at 6 mL/s through an 18 G intravenous antecubital catheter using a dual-syringe injector (Stellant D, Medrad, Indianola, PA). The study acquisition delay time was estimated by injection of a 15 mL contrast medium test bolus at 6 mL/s, followed by 50 mL of saline. The actual delay time was calculated as the time of peak contrast medium attenuation in a region of interest in the ascending aorta plus 4 seconds. For prospectively ECG-triggered coronary CT angiography, acquisition parameters were 2 × 64 × 0.6 mm detector collimation resulting in 2 × 128 × 0.6 mm sections, 280 ms gantry rotation time, and 320 mAs per rotation tube current time product. A 120 kV tube potential was used, becauseall 10 patients had a body mass index of >25 kg/m^2. Acquisition was cranio-caudal from above the origin of the coronary arteries to below the dome of the diaphragm. Adaptive prospective ECG-triggering was used with the full radiation dose window set at 70% of the R-R′ interval in patients with heart rates ≤70 beats per minute (bpm), and 40% of the R-R′ interval in patients with a heart rate of >70 bpm. Reduced dose (20% of the nominal tube current) was applied between 30% and 90% of the R-R′ interval to obtain functional information during these cardiac phases. For coronary artery evaluation datasets were reconstructed using 0.75 mm section thickness and 0.3 mm reconstruction increment at 40% or 70% R-R′ depending on the heart rate. An additional reconstruction was performed during systole at 250 ms after the R-peak to plan the coverage range for the myocardial perfusion acquisition.

Myocardial perfusion imaging was performed using a dynamic acquisition mode 3 minutes into adenosine (140 μg/kg/min) stress. Data were acquired during every other R-R′ interval at 2 alternating table positions in ECG-triggered mode during end systole (250 ms after the R-peak), with the table shuttling back and forth between the 2 positions (table acceleration: 300 mm/s^2) during image acquisition. A complete dataset of the whole cardiac volume was acquired every ~2.8 seconds. Given a detector width of 38 mm, and a 10% overlap between both acquisition ranges, the anatomic coverage of this imaging technique is 73 mm. Image acquisition parameters were 100 kV tube voltage and 300 mAs. The image acquisition sequence was initiated 4 seconds before the arrival of the contrast medium bolus front as determined by the initial test bolus injection to ensure baseline acquisition of noncontrast images before the onset of first-pass perfusion. Myocardial perfusion studies were contrast medium enhanced with 50 mL of iopromide, followed by 50 mL of saline, injected at 6 mL/s. Including test bolus acquisition and coronary CTA angiography, each patient thus received a total volume of 150 mL contrast medium and 135 mL saline. Studies were obtained during end-inspiration with a standardized acquisition time of 30 seconds. If patients could not hold their breath for 30 seconds, they were instructed to slowly release their breath and continue breathing shallowly. Images were reconstructed with 3 mm slice width every 2 mm with a medium sharpness convolution algorithm and then processed using the Volume Perfusion software (syngo VA31, Siemens).

Finally, delayed enhancement studies were performed 6 minutes after perfusion imaging using a regular prospectively ECG-triggered mode with image acquisition at 70% of the R-R′ interval at 80 kV and 320 mAs. For delayed enhancement imaging, no functional image information was acquired.

Perfusion Data Analysis

Two experienced radiologists independently evaluated MRI and CT studies blinded to clinical history. CT and MRI data were evaluated separately and in random order. Discordant findings were reconciled during a consensus read.

For qualitative analysis dynamic stress CT perfusion and MRI studies were interpreted visually in conjunction with delayed enhancement CT and MRI viability scans. On both, CT and MRI, a myocardial segment was considered as showing reversible ischemia when hypoperfusion lasted for more than 6 heart beats under adenosine stress without delayed enhancement on viability scans. Myocardial perfusion defects were classified as fixed if the hypoattenuation lasted for more than 6 heart beats under adenosine stress and delayed enhancement was seen on viability scans. Homogeneously perfused myocardium during adenosine stress that did not show delayed enhancement on viability studies was classified as normal.[18]

Semi quantitative perfusion analysis was performed on 10 mm slice thickness short-axis multiplanar reformats of the stress cardiac CT acquisitions, representative of basal, mid, and apical portions of the left ventricular myocardium as well as on the 3 short-axis sections acquired at stress perfusion MRI. A commercially available software application (Argus, Siemens) was used for this purpose for both, CT and MRI studies. CT and MRI studies were evaluated in random order using the 16-segment American Heart Association model.[19] The segments were automatically traced by the software after epicardial and endocardial borders were manually defined. Semi quantitative perfusion analysis was based on computing the upslope of the signal intensity over time curve from unenhanced myocardium to maximum signal intensity during the myocardial first pass of the contrast agent, according to the "myocardial-to-left ventricular upslope index" method.[20] All parameters were normalized to blood pool signal intensity curves.[20,21]

Absolute myocardial perfusion quantification was performed based on dynamic perfusion CT studies using a prototype version of the Volume Perfusion software (syngo VA31, Siemens). A dedicated parametric deconvolution technique based on a 2 compartment model of intra- and extravascular space was used to fit the time attenuation curves. For increasing the precision of the fit, double sampling of the arterial input function (AIF) was performed. The input function was sampled in the descending aorta at every table position and combined into one AIF that had twice the sampling rate of the tissue time-attenuation-curve (TAC). The algorithm then determined the maximum slope from the fit model curve for every voxel and calculated myocardial blood flow (MBF) according to the following relationship: MBF = Max Slope (TissueTAC)/Maximum (AIF), where the maximum slope reflects the tissue TAC and the maximum (AIF) indicates the maximum AIF value.

balt6/z7l-ir/z7l-ir/z7l00610/z7l3090-10z | xppws | S=1 | 4/2/10 | 3:36 | 4/Color Figure(s): F1-3 | Art: RLI200544

Statistical Analysis

Data are expressed as mean ± SD. Interobserver agreement for visual assessment of myocardial perfusion defects was calculated with Cohen kappa statistics,[22] and interpreted as follows: less than 0.20, slight or poor agreement; 0.20 to 0.40, fair agreement; 0.41 to 0.80, moderate agreement; greater than 0.80, excellent agreement. Qualitative estimation of perfusion CT and MRI were compared on a per-segment basis to determine sensitivity, specificity, positive and negative predictive values for the detection of myocardial perfusion defects. Dynamic first-pass perfusion results were evaluated using paired Student *t* test or Wilcoxon signed-rank test, where appropriate. Bland-Altman analysis was performed to determine agreement between the upslopes of myocardial signal intensity curves estimated by CT and MRI. Spearman's coefficient of rank correlation (rho) was calculated to assess correlation between dynamic perfusion CT-derived myocardial signal intensity upslope and MBF and interpreted as follows: 0 to 0.1: very low, 0.11 to 0.30: low, 0.31 to 0.5: moderate, 0.51 to 0.7: high, 0.71 to 0.9: very high, 0.91 to 1: almost perfect. A P level <0.05 indicated a statistically significant difference. Data analysis was performed with commercially available statistical software packages (WINPEPI, version 8.8, PEPI-for-Windows; MedCalc, Version 9.3.0.0. MedCalc Software; Mariakerke, Belgium, and SPSS for Windows, version 15.0, SPSS Inc., Chicago, IL).

RESULTS

Clinical Characteristics of the Patient Population

All study procedures were successfully completed in all subjects, without any adverse events. Demographic characteristics of the study population are shown in Table 1. The mean age of the 10 subjects (8 male, 2 female) included in the study was 62.7 ± 7.1 years (range, 51–71 years). Subjects′ mean heart rates during rest and under adenosine-induced stress did not significantly differ between CT and MRI exams. Mean total dose length product (DLP) of the 4 components (calcium scoring, coronary CT angiography, perfusion, delayed enhancement) of the cardiac CT protocol was 1290.4 ± 233.3 mGy cm (range, 935–1776 mGy cm). The dynamic CT perfusion study by itself resulted in a mean DLP of 733.5 ± 139.6 mGy cm (range, 508–971 mGy cm).

TABLE 1. Patient Demographics

Population	
No. patients	10
Age (yr) (mean ± SD; range)	62.7 ± 7.1 (51–71)
Gender (M/F)	8/2
Heart rate (bpm) (mean ± SD; range)	
Rest CT	63 ± 12.1 (53–95)
Stress CT	75.3 ± 16.7 (55–102)
Rest MRI	61.2 ± 11.7 (50–89)
Stress MRI	69.2 ± 11.8 (52–90)
History	
No known coronary artery disease	5 (50%)
Previous myocardial infarction	4 (40%)
PTCA without stent placement	2 (20%)
PTCA with stent placement	2 (20%)
Bypass	2 (20%)
Cardiovascular risk factors	
Hypertension (%)	10 (100%)
Dyslipidemia (%)	10 (100%)
Diabetes (%)	1 (10%)
Smoking (%)	3 (30%)
Family history (%)	4 (40%)
BMI (kg/m^2; mean ± SD; range)	30.8 ± 5.6 (25.1–41.5)

SD indicates standard deviation; bpm, beats per minute; PTCA, percutaneous transluminal coronary angioplasty; BMI, body mass index.

Coronary CT Angiography

Evaluation of coronary CT angiograms ruled out significant coronary artery stenosis in 4 patients (Fig. 1). Coronary CT angiograms showed occlusion of the distal right coronary artery (RCA) in one patient (Fig. 2), significant stenosis of the proximal circumflex artery (Cx) in another patient, and significant stenosis of the distal RCA in a third patient (Fig. 3). In the 2 subjects with prior bypass surgery, one showed occlusion of a left internal mammary artery to left anterior descending coronary artery (LAD) graft and the second patient had occlusion of the LAD distal to the left internal mammary artery graft anastomosis. In the 2 patients with prior stent placement (one of them also had a bypass), all stents (n = 3) were patent on coronary CT angiography. Overall, 5 patients had significant coronary artery stenosis on coronary CT angiography.

Qualitative Assessment of Myocardial Perfusion

Seven segments in 4 patients were excluded from analysis because oflimited anatomic coverage of the dynamic CT perfusion acquisition mode (segment 1 in 3 patients, segment 6 in 2 patients, and segments 7 and 12 in one patient). Artifacts on one stress MRI study prohibited adequate assessment of the apical segments of the left ventricle in one patient (segments 13–16). Therefore, a total of 149 segments (93.1%) were included for analysis.

Interobserver agreement for detecting myocardial perfusion defects on CT and MRI was excellent (k = 0.85 and k = 0.86, respectively). Visual assessment of MRI perfusion studies showed perfusion defects in 36 myocardial segments (39.1%) in 6 patients. Twenty-nine of these perfusion defects were fixed whereas 7 represented reversible ischemia. Dynamic stress CT perfusion correctly classified 31 of these perfusion defects but missed 5 (2 reversible) detected on MRI (Table 2). Overall, dynamic perfusion CT had 86.1% (71.3%–93.9%) sensitivity, 98.2% (93.8%–99.5%) specificity, 93.9% (81.8%–98.2%) positive predictive value, and 95.7% (91%–97.9%) negative predictive value in comparison with perfusion MRI for detecting any type of myocardial perfusion defect on a segmental basis.

Semiquantitative Assessment of Myocardial Perfusion

At dynamic stress perfusion CT, estimation of the upslope of the signal intensity over time curve between normal (5.4 ± 2.1 SI/s) and hypoperfused (4.4 ± 1.5 SI/s) myocardium showed significant differences ($P = 0.01$). These differences were also significant in stress MRI studies (5.1 ± 2.2 SI/s and 3.8 ± 2 SI/s, respectively, $P < 0.01$) (Fig. 4). The difference between CT and MRI data for differentiating normal and hypoperfused myocardial segments was not statistically significant ($P = 0.79$). Overall, when dynamic stress perfusion CT and semi quantitative stress perfusion MRI data were compared, no statistically significant difference was observed for the upslope of the signal intensity over time curve (4.8 ± 2.3 SI/s for MRI and 5.2 ± 2 SI/s for CT) (Fig. 5), with dynamic CT mildly overestimating the upslope (mean difference of 0.3, 95% confidence limits of agreement: 0–0.7) (Fig. 6). Comparison of this parameter showed similar results when normal and hypoperfused myocardial segments were compared separately.

balt6/z7l-ir/z7l-ir/z7l00610/z7l3090-10z | xppws | S=1 | 4/2/10 | 3:36 | 4/Color Figure(s): F1-3 | Art: RLI200544

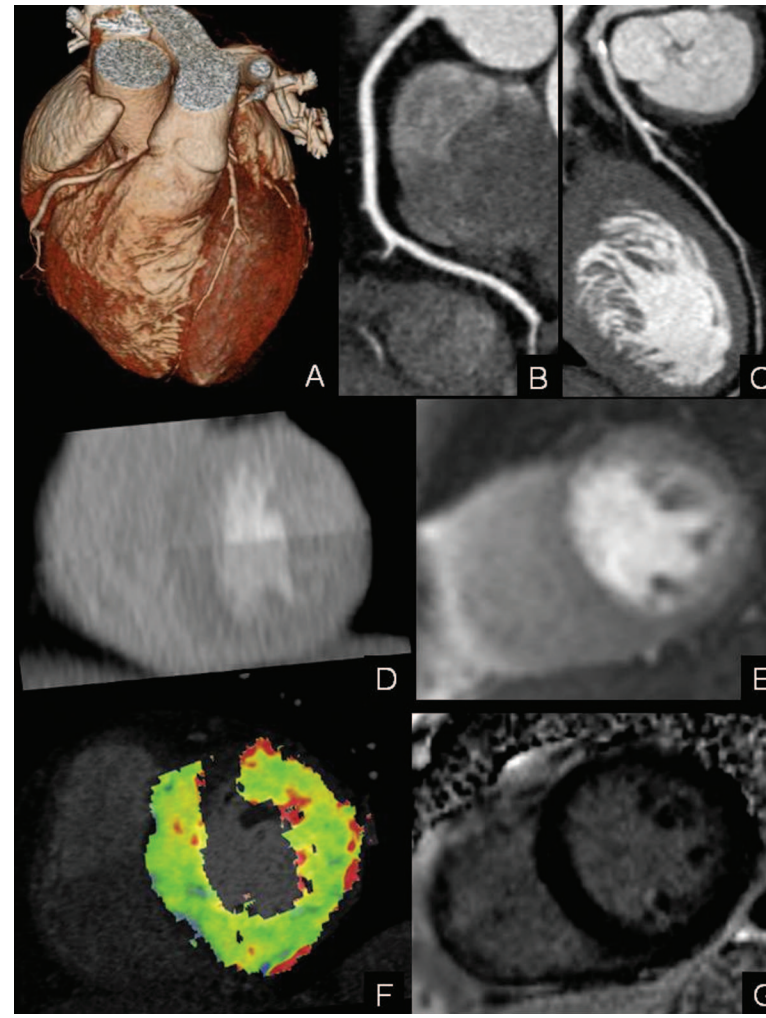

FIGURE 1. A 66-year-old woman with hypertension, dyslipidemia, and chest pain. A, Volume rendered coronary CT angiography study. Curved multiplanar reformats of the RCA (B) and LAD (C) show eccentric calcification of the LAD but no significant stenosis. Dynamic stress perfusion CT (D) as well as stress MRI (E) show normal myocardial perfusion. The CT myocardial perfusion map (F) reveals homogenous myocardial perfusion. Delayed acquisition MRI study (G) does not show late enhancement of the myocardium.

Quantitative Assessment of CT Myocardial Perfusion

Mean MBF of all myocardial segments at dynamic stress perfusion CT was 115.9 ± 46.5 mL/100 mL/min (range, 43.1–277.8 mL/100 mL/min). There was a significant difference in MBF values between normal (122.2 ± 49.4 mL/100 mL/min) and hypoperfused (96 ± 27.9 mL/100 mL/min) myocardial segments ($P < 0.001$). Overall, moderate correlation was observed between absolute MBF quantification at dynamic perfusion CT and the upslope of the perfusion CT-derived signal intensity over time curves ($r = 0.47$, $P < 0.01$). Correlation between MBF and semiquantitative upslope values was also moderate for hypoperfused ($r = 0.41$, $P < 0.01$) and normal myocardial segments ($r = 0.43$, $P < 0.01$).

DISCUSSION

This study demonstrates that adenosine-stress dynamic volume CT perfusion is feasible and may enable the qualitative and semi quantitative assessment of myocardial perfusion parameters in a comparable fashion as MRI in patients with suspected or known coronary artery disease.

Improved temporal resolution together with high spatial resolution of contemporary MRI technology has reinvigorated the use of first-pass perfusion MRI for assessing the hemodynamic significance of coronary artery stenosis. At the same time comprehensive evaluation of coronary artery disease by means of a single examination capable of addressing most clinically relevant aspects of coronary heart disease, including detection of stenoses and evaluation of their effect on cardiac function, perfusion, and viability has become a major objective of cardiac MDCT imaging research.[11–13,15,23,24] Moreover, myocardial tissue kinetics of iodine contrast agents and gadolinium chelates are similar,[25] a fact that may add clinical justification to research efforts aimed at CT myocardial perfusion imaging.

Appropriate visualization of first-pass myocardial perfusion, however, requires time-resolved volume image acquisition during the infusion of contrast medium. The technical prerequisites for this application for use with mechanical MDCT technology have only recently been fulfilled by the introduction of wide detector array CT[13,26,27] and new DSCT systems.[16,17] Unlike previous generation MDCT scanners with narrower detectors, these latter instruments enable dynamic time-resolved perfusion imaging in a larger myocardial volume thus overcoming the main limitations of previous generation MDCT systems. With earlier MDCT scanner generations, estimation of myocardial perfusion relied on the analysis of myocardial attenuation only during a single discrete phase of arterial contrast enhancement without time-resolved evaluation of myocardial contrast kinetics,[12] while actual myocardial first-pass perfusion imaging, was restricted to a limited portion of the

balt6/z7l-ir/z7l-ir/z7l00610/z7l3090-10z | xppws | S=1 | 4/2/10 | 3:36 | 4/Color Figure(s): F1-3 | Art: RLI200544

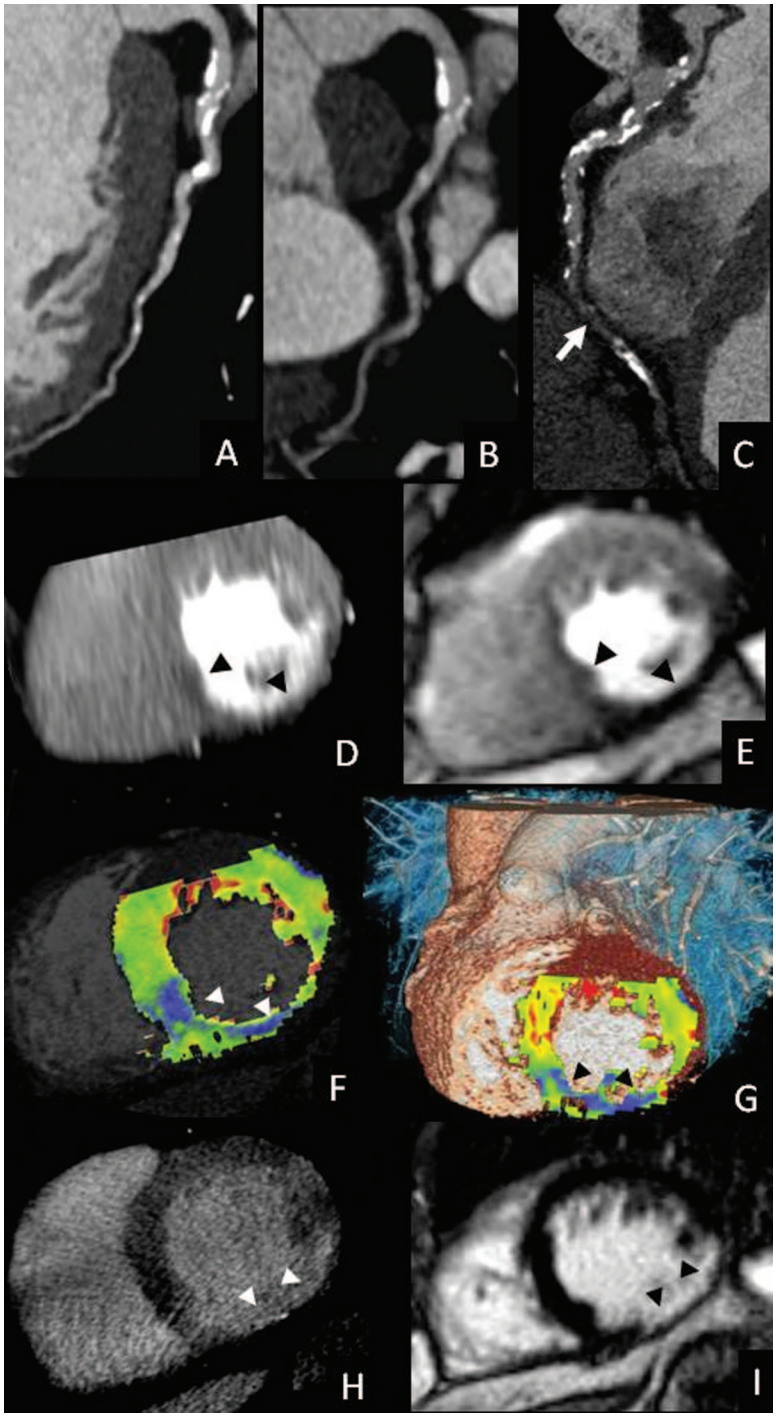

FIGURE 2. A 64-year-old man with history of smoking, hypertension, dyslipidemia, and prior inferior myocardial infarction treated with percutaneous transluminal coronary angioplasty. Curved multiplanar reformats of the LAD (A), Cx (B) and RCA (C) show extensive atherosclerotic disease with distal RCA occlusion (arrow in C). Visual assessment of dynamic CT perfusion (D) reveals inferior and inferoseptal perfusion defects (arrowheads), confirmed by MRI (E). Absolute MBF images (F, G) map the perfusion defects visualized during first-pass perfusion (arrowheads), which correspond to the known chronic inferior myocardial infarction with inferoseptal peri-infarct ischemia, as established by delayed enhancement CT (H, arrowheads) and MRI (I, arrowheads).

myocardium because ofinsufficient volume coverage along the z-axis of the heart.[28,29]

As shown in this study, dynamic first-pass myocardial CT perfusion imaging provides comparable results as MRI for classification of myocardial tissue as normal and ischemic, and for determining semi quantitative parameters of myocardial blood flow. Our results indicate high specificity and negative predictive values for the qualitative assessment of myocardial perfusion, with a low rate of false-positive findings. When myocardial perfusion was semi quantitatively analyzed, dynamic perfusion CT could differentiate between healthy and diseased myocardium in a comparable fashion as MRI by computing the signal intensity over time curve. Furthermore, the upslope values were not significantly different when dynamic CT- and MRI-derived measurements were compared. Therefore, in line with MRI observations where the myocardial signal intensity upslope has been proposed as the most reliable semi quantitative parameter for estimating myocardial perfusion for clinical purposes,[30,31] our results support the validity of this parameter also for semiquantitative assessment of myocardial perfusion based on dynamic CT. Lastly, our results suggest the feasibility of using

balt6/z7l-ir/z7l-ir/z7l00610/z7l3090-10z | xppws | S=1 | 4/2/10 | 3:36 | 4/Color Figure(s): F1-3 | Art: RLI200544

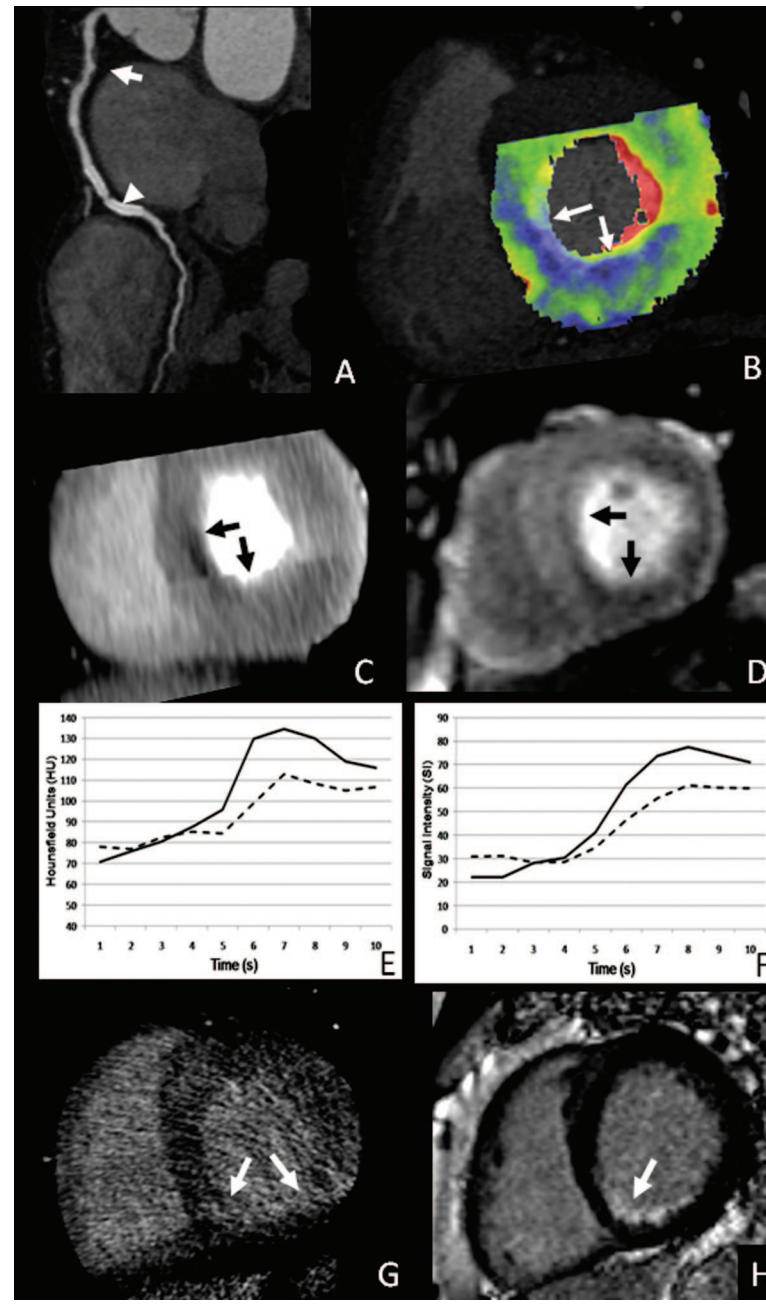

FIGURE 3. A 51-year-old man with history of inferoseptal myocardial infarction and prior RCA stent placement. A, Curved multiplanar reformat of the RCA shows noncalcified plaque causing luminal irregularities (arrow) of the proximal RCA, 2 patent stents, and significant stenosis (arrowhead) of the RCA segment between the 2 stents. The CT myocardial blood pool perfusion map (B) reveals hypoperfusion of the basal inferior, inferoseptal and septal myocardial segments (arrows) consistent with fixed defects corresponding to chronic infarction and septal peri-infarct ischemia. Visual assessment of stress dynamic CT perfusion (C) and stress MRI (D) show hypo-perfusion in the ischemic and infarcted territory (arrows), Semi quantitative analysis results in comparable myocardial perfusion curves for CT (E) and MRI (F) in septal myocardium with reversible ischemia (dashed lines) and healthy lateral myocardium (solid lines), confirmed by delayed enhancement CT (G) and MRI (H).

TABLE 2. Qualitative Analysis of Myocardial Perfusion by Stress Dynamic CT and MRI on a Per-Segment Basis

	MRI	
	Positive	**Negative**
CT		
Positive	31	2
Negative	5	111

dynamic first-pass perfusion CT to obtain absolute quantitative parameters of myocardial blood-flow. As previously shown for MRI[20] and in line with recent experimental myocardial CT perfusion study findings,[11] we observed moderate correlation between absolute MBF quantification and the upslope of the signal intensity over time curve.

There are several limitations to our study. First, the acquisition coverage of 73 mm was insufficient for encompassing the entire heart in 4 of our patients, thus precluding analysis of some myocardial segments. Further improvements in CT technology should aim at providing greater coverage along the z-axis to approach that of latest generation single-source CT systems.[26] Second, the total injected volume of intravenous iodinated contrast material was higher than for conventional cardiac CT examinations, but within the ranges of the amount of contrast medium routinely administered for regular body CT examinations. Third, addition of a dynamic CT perfusion acquisition to a conventional coronary CT angiogram

balt6/z7l-ir/z7l-ir/z7l00610/z7l3090-10z | xppws | S=1 | 4/2/10 | 3:36 | 4/Color Figure(s): F1-3 | Art: RLI200544

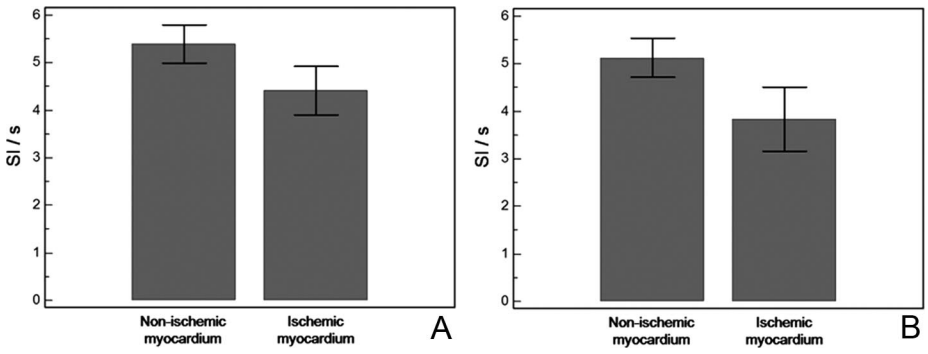

FIGURE 4. Differences in the upslope of the signal intensity over time curve mean values between healthy and diseased myocardium as assessed by stress perfusion CT (A) and MRI (B). Significant differences were observed in myocardial signal intensity upslope values between normal and hypo-perfused myocardium both with CT (5.4 ± 2.1 UH/s vs. 4.4 ± 1.5 UH/s) and MRI (5.1 ± 2.2 SI/s vs. 3.8 ± 2 SI/s). Error bars represent 95% confidence interval for the mean.

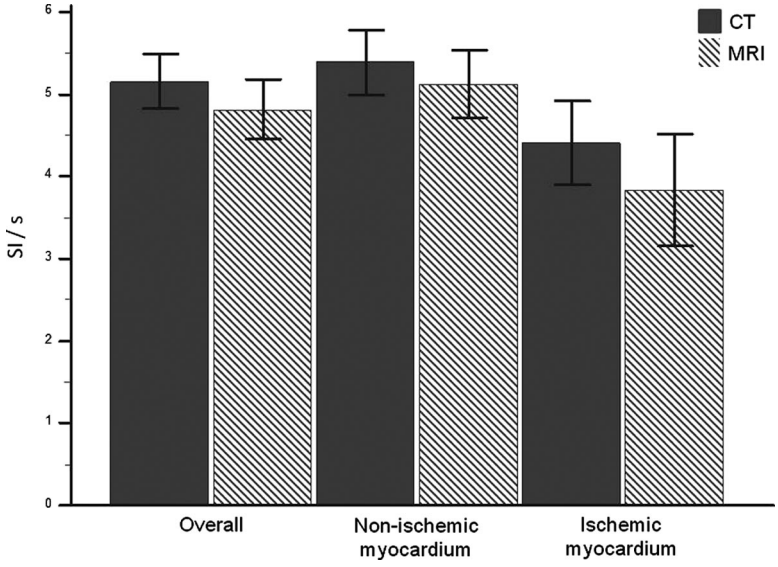

FIGURE 5. Comparison of stress-induced myocardial perfusion upslope of the signal intensity over time curve between dynamic CT perfusion and MRI. No statistically significant differences were observed between CT and MRI measurements for each variable (overall $P = 0.07$, nonischemic myocardium $P = 0.23$, ischemic myocardium $P = 0.11$).

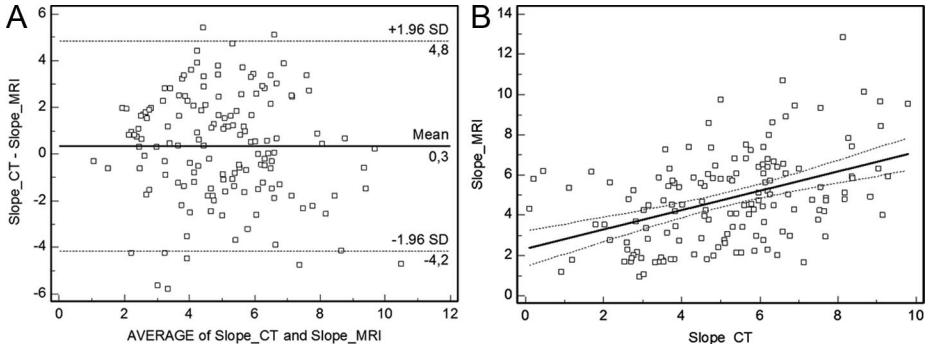

FIGURE 6. Bland-Altman analysis (A) and correlation graph (B) comparing agreement and correlation between stress CT and MRI derived upslope of the signal intensity over time curves.

entails an increase in radiation dose. According to this preliminary experience, however, the total amount of radiation patients received from our integrative cardiac CT protocol was within the range of values described for regular retrospectively ECG-gated coronary CT angiography[32] and equivalent to the radiation dose from single photon emission computed tomography procedures.[33] Therefore, although, different from MRI, this method involves radiation, it may become an option for patients with MRI contraindications and for patients in whom simultaneous assessment for coronary artery stenosis is desired. Fourth, dynamic CT myocardial perfusion has substantially lower temporal resolution than MRI perfusion imaging. This, however, evidently did not detrimentally interfere with the estimation of semi quantitative myocardial perfusion as compared with MRI. Lastly, following current trends in nuclear[34] and MRI myocardial perfusion imaging[35] and to avoid excessive radiation exposure, our cardiac CT study protocol included stress perfusion only. Accordingly, based on stress CT imaging alone, we cannot differentiate between fixed and reversible perfusion defects. However, the differentiation between infarct and ischemia is enabled by synopsis with delayed enhancement CT and possibly with coronary CT angiography prior to stress perfusion, which may serve as a surrogate in lieu of a dedicated rest perfusion acquisition.

In conclusion, we demonstrate that adenosine-stress dynamic perfusion CT is technically feasible and can differentiate between

healthy and diseased myocardium. This technique enables visual and semi quantitative assessment of perfusion parameters in a comparable fashion as MRI. These findings may serve to further emphasize the potential of CT for integrative imaging of all pertinent aspects of coronary heart disease, including coronary artery morphology, cardiac function, perfusion, and viability with a single modality.

REFERENCES

1. Hendel RC, Berman DS, Di Carli MF, et al. ACCF/ASNC/ACR/AHA/ASE/SCCT/SCMR/SNM 2009 appropriate use criteria for cardiac radionuclide imaging: a report of the American College of Cardiology Foundation Appropriate Use Criteria Task Force, the American Society of Nuclear Cardiology, the American College of Radiology, the American Heart Association, the American Society of Echocardiography, the Society of Cardiovascular Computed Tomography, the Society for Cardiovascular Magnetic Resonance, and the Society of Nuclear Medicine: endorsed by the American College of Emergency Physicians. *Circulation*. 2009;119:e561–e587.
2. Hendel RC, Patel MR, Kramer CM, et al. ACCF/ACR/SCCT/SCMR/ASNC/NASCI/SCAI/SIR 2006 appropriateness criteria for cardiac computed tomography and cardiac magnetic resonance imaging: a report of the American College of Cardiology Foundation Quality Strategic Directions Committee Appropriateness Criteria Working Group, American College of Radiology, Society of Cardiovascular Computed Tomography, Society for Cardiovascular Magnetic Resonance, American Society of Nuclear Cardiology, North American Society for Cardiac Imaging, Society for Cardiovascular Angiography and Interventions, and Society of Interventional Radiology. *J Am Coll Cardiol*. 2006;48:1475–1497.
3. Schwitter J, Wacker CM, van Rossum AC, et al. MR-IMPACT: comparison of perfusion-cardiac magnetic resonance with single-photon emission computed tomography for the detection of coronary artery disease in a multicentre, multivendor, randomized trial. *Eur Heart J*. 2008;29:480–489.
4. Brodoefel H, Burgstahler C, Tsiflikas I, et al. Dual-source CT: effect of heart rate, heart rate variability, and calcification on image quality and diagnostic accuracy. *Radiology*. 2008;247:346–355.
5. Meijboom WB, Meijs MF, Schuijf JD, et al. Diagnostic accuracy of 64-slice computed tomography coronary angiography: a prospective, multicenter, multivendor study. *J Am Coll Cardiol*. 2008;52:2135–2144.
6. Miller JM, Rochitte CE, Dewey M, et al. Diagnostic performance of coronary angiography by 64-row CT. *N Engl J Med*. 2008;359:2324–2336.
7. Carrigan TP, Nair D, Schoenhagen P, et al. Prognostic utility of 64-slice computed tomography in patients with suspected but no documented coronary artery disease. *Eur Heart J*. 2009;30:362–371.
8. Gopal A, Nasir K, Ahmadi N, et al. Cardiac computed tomographic angiography in an outpatient setting: an analysis of clinical outcomes over a 40-month period. *J Cardiovasc Comput Tomogr*. 2009;3:90–95.
9. Hadamitzky M, Freissmuth B, Meyer T, et al. Prognostic value of coronary computed tomographic angiography for prediction of cardiac events in patients with suspected coronary artery disease. *JACC Cardiovasc Imaging*. 2009;2:404–411.
10. Min JK, Shaw LJ, Devereux RB, et al. Prognostic value of multidetector coronary computed tomographic angiography for prediction of all-cause mortality. *J Am Coll Cardiol*. 2007;50:1161–1170.
11. George RT, Jerosch-Herold M, Silva C, et al. Quantification of myocardial perfusion using dynamic 64-detector computed tomography. *Invest Radiol*. 2007;42:815–822.
12. George RT, Silva C, Cordeiro MA, et al. Multidetector computed tomography myocardial perfusion imaging during adenosine stress. *J Am Coll Cardiol*. 2006;48:153–160.
13. George RT, Arbab-Zadeh A, Miller JM, et al. Adenosine stress 64- and 256-row detector computed tomography angiography and perfusion imaging: a pilot study evaluating the transmural extent of perfusion abnormalities to predict atherosclerosis causing myocardial ischemia. *Circ Cardiovasc Imaging*. 2009;2:174–182.
14. Ruzsics B, Lee H, Zwerner PL, et al. Dual-energy CT of the heart for diagnosing coronary artery stenosis and myocardial ischemia-initial experience. *Eur Radiol*. 2008;18:2414–2424.
15. Ruzsics B, Schwarz F, Schoepf UJ, et al. Comparison of dual-energy computed tomography of the heart with single photon emission computed tomography for assessment of coronary artery stenosis and of the myocardial blood supply. *Am J Cardiol*. 2009;104:318–326.
16. Lell M, Marwan M, Schepis T, et al. Prospectively ECG-triggered high-pitch spiral acquisition for coronary CT angiography using dual source CT: technique and initial experience. *Eur Radiol*. 2009;19:2576–2583.
17. Leschka S, Stolzmann P, Desbiolles L, et al. Diagnostic accuracy of high-pitch dual-source CT for the assessment of coronary stenoses: first experience. *Eur Radiol*. 2009;19:2896–2903.
18. Plein S, Ryf S, Schwitter J, et al. Dynamic contrast-enhanced myocardial perfusion MRI accelerated with k-t sense. *Magn Reson Med*. 2007;58:777–785.
19. Cerqueira MD, Weissman NJ, Dilsizian V, et al. Standardized myocardial segmentation and nomenclature for tomographic imaging of the heart: a statement for healthcare professionals from the Cardiac Imaging Committee of the Council on Clinical Cardiology of the American Heart Association. *Circulation*. 2002;105:539–542.
20. Christian TF, Rettmann DW, Aletras AH, et al. Absolute myocardial perfusion in canines measured by using dual-bolus first-pass MR imaging. *Radiology*. 2004;232:677–684.
21. Nagel E, Klein C, Paetsch I, et al. Magnetic resonance perfusion measurements for the noninvasive detection of coronary artery disease. *Circulation*. 2003;108:432–437.
22. Cohen J. A coefficient of agreement for nominal scales. *Educ Psychol Meas*. 1960;20:37–46.
23. Blankstein R, Shturman LD, Rogers IS, et al. Adenosine-induced stress myocardial perfusion imaging using dual-source cardiac computed tomography. *J Am Coll Cardiol*. 2009;54:1072–1084.
24. Rocha-Filho JA, Blankstein R, Shturman LD, et al. Incremental value of adenosine-induced stress myocardial perfusion imaging with dual-source CT at cardiac CT angiography. *Radiology*. 2010;254:410–419.
25. Gerber BL, Belge B, Legros GJ, et al. Characterization of acute and chronic myocardial infarcts by multidetector computed tomography: comparison with contrast-enhanced magnetic resonance. *Circulation*. 2006;113:823–833.
26. Dewey M, Zimmermann E, Deissenrieder F, et al. Noninvasive coronary angiography by 320-row computed tomography with lower radiation exposure and maintained diagnostic accuracy: comparison of results with cardiac catheterization in a head-to-head pilot investigation. *Circulation*. 2009;120:867–875.
27. Flohr TG, Bruder H, Stierstorfer K, et al. Image reconstruction and image quality evaluation for a dual source CT scanner. *Med Phys*. 2008;35:5882–5897.
28. Mahnken AH, Bruners P, Katoh M, et al. Dynamic multi-section CT imaging in acute myocardial infarction: preliminary animal experience. *Eur Radiol*. 2006;16:746–752.
29. Kido T, Kurata A, Higashino H, et al. Quantification of regional myocardial blood flow using first-pass multidetector-row computed tomography and adenosine triphosphate in coronary artery disease. *Circ J*. 2008;72:1086–1091.
30. Schwitter J, Nanz D, Kneifel S, et al. Assessment of myocardial perfusion in coronary artery disease by magnetic resonance: a comparison with positron emission tomography and coronary angiography. *Circulation*. 2001;103:2230–2235.
31. Al-Saadi N, Nagel E, Gross M, et al. Noninvasive detection of myocardial ischemia from perfusion reserve based on cardiovascular magnetic resonance. *Circulation*. 2000;101:1379–1383.
32. Stolzmann P, Scheffel H, Schertler T, et al. Radiation dose estimates in dual-source computed tomography coronary angiography. *Eur Radiol*. 2008;18:592–599.
33. Gerber TC, Carr JJ, Arai AE, et al. Ionizing radiation in cardiac imaging: a science advisory from the American Heart Association Committee on Cardiac Imaging of the Council on Clinical Cardiology and Committee on Cardiovascular Imaging and Intervention of the Council on Cardiovascular Radiology and Intervention. *Circulation*. 2009;119:1056–1065.
34. Chang SM, Nabi F, Xu J, et al. Normal stress-only versus standard stress/rest myocardial perfusion imaging: similar patient mortality with reduced radiation exposure. *J Am Coll Cardiol*. 2010;55:221–230.
35. Krittayaphong R, Boonyasirinant T, Saiviroonporn P, et al. Myocardial perfusion cardiac magnetic resonance for the diagnosis of coronary artery disease: do we need rest images? *Int J Cardiovasc Imaging*. 2009;25(suppl 1):139–148.

AUTHOR QUERIES

AUTHOR PLEASE ANSWER ALL QUERIES **1**

AQ1—Please check whether the short title is OK as given.

AQ2—Please check whether the layout of Table 2 is OK.